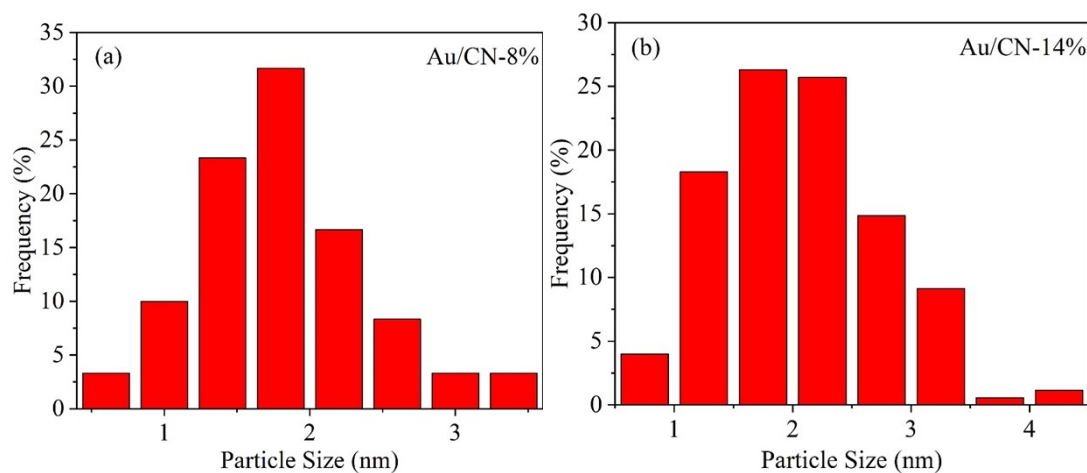


## Materials

KOH ( $\cong 85.0\%$ ), urea ( $\cong 99.0\%$ ),  $\text{KHCO}_3$  ( $\cong 99.5\%$ ),  $\text{Na}_2\text{SO}_4$  ( $\cong 99.0\%$ ),  $\text{NaBH}_4$  ( $\cong 98.0\%$ ), HCl (36.0~38.0%),  $\text{HNO}_3$  (65.0~68.0%), ethanol ( $\cong 99.7\%$ );  $\text{HClO}_4$  (70.0%-72.0%) and  $\text{HAuCl}_4$  ( $\cong 99.9\%$ ) was purchased from Shanghai Lingfeng and Shanghai Chemical Reagent Co., Ltd; Nafion solution (5 wt%) was purchased from Dupont; anion exchange membrane (Fumasep<sup>®</sup> FAA-3-50), carbon black (Vulcan XC 72R) and Toray Carbon Paper (TGP-H-60) was purchased via Fuel Cell Store website. All other chemicals were purchased from Sinopharm Chemical Reagent Co., Ltd. Milli-Q ultrapure water (Millipore,  $\geq 18 \text{ M}\Omega/\text{cm}$ ) was used throughout the work.

## Characterizations

The physical morphologies of the Au catalysts supported on N-doped carbon were examined by transmission electron microscopy (TEM, Hitachi HT7700). The phase identification of the materials was carried out using an X-ray diffraction (Haoyuan, DX-27mini). The X-ray photoelectron spectroscopy (Thermo ESCALAB 250XI) measurement was performed for C1s, Au4f, N1s spectra. The actual mass ratio of gold in the catalyst was determined by inductively coupled plasma emission spectrometer (ICP, Optima8300DV). The morphologies of the cathode materials were analyzed by scanning electron microscopy (SEM, Hitachi TM3030).



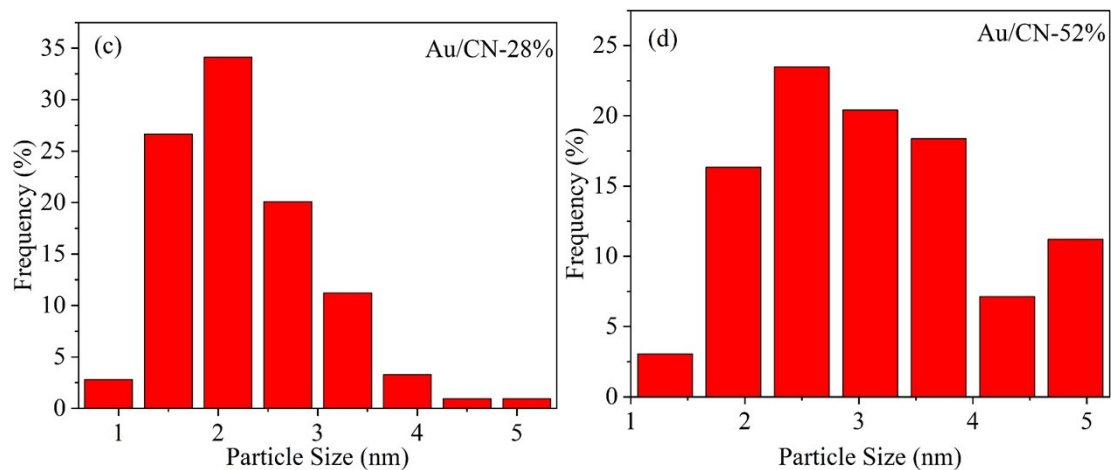


**Figure S1.** (a)-(d) Histograms of Au nanoparticles size distribution extracted from TEM images of the four samples.

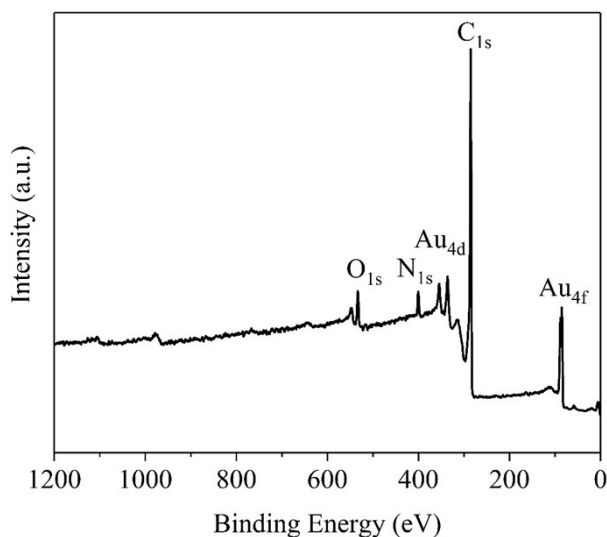


**Figure S2.** XPS survey of Au/CN-14%.

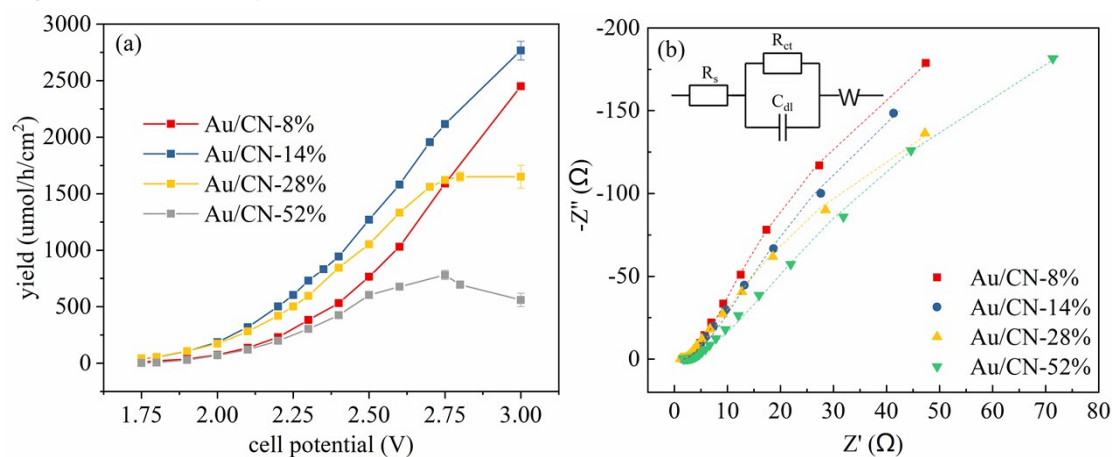


**Figure S3.** (a) The CO yielding under different cell potential at the self-made CO<sub>2</sub> electrolyzer; (b) electrochemical impedance spectroscopy and the relevant equivalent circuit of Au/CN catalyst measured in CO<sub>2</sub> electrolyser at open circuit.

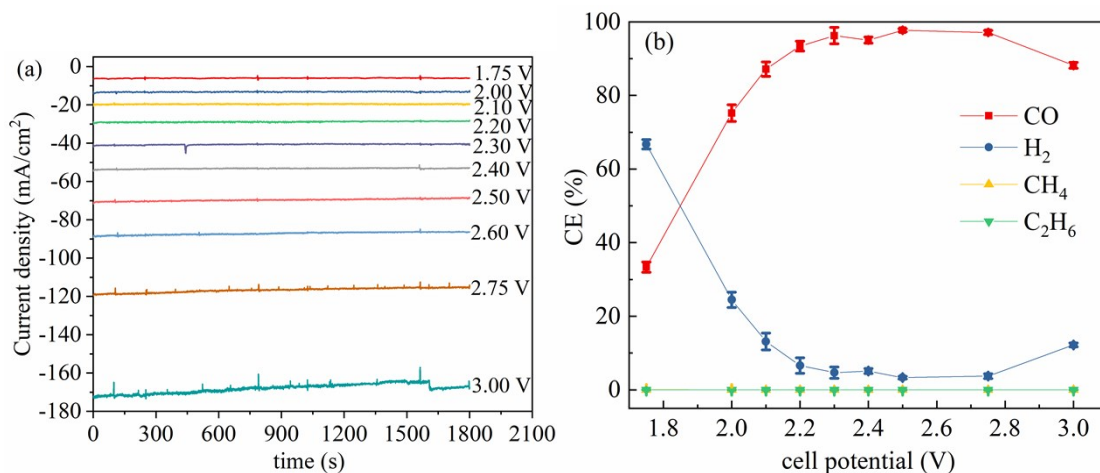


**Figure S4.** Total current density as a function of time under different cell potential; (b) current efficiency of gas productions, as a function of the cell potential. Cathode: Au/CN-14%.

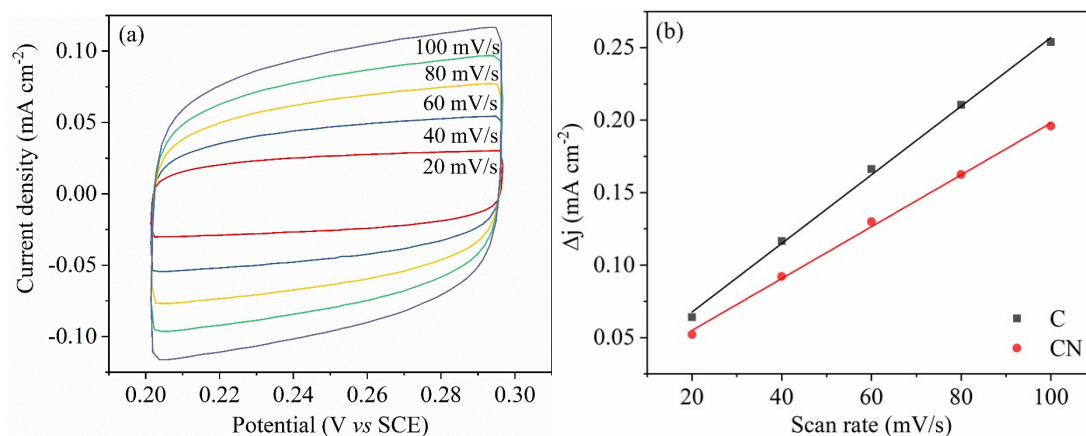


**Figure S5.** (a) CV curves of pure C measured at different scan rates in 0.1 M Na<sub>2</sub>SO<sub>4</sub> solution; (b) charging current differences plotted against scan rate.

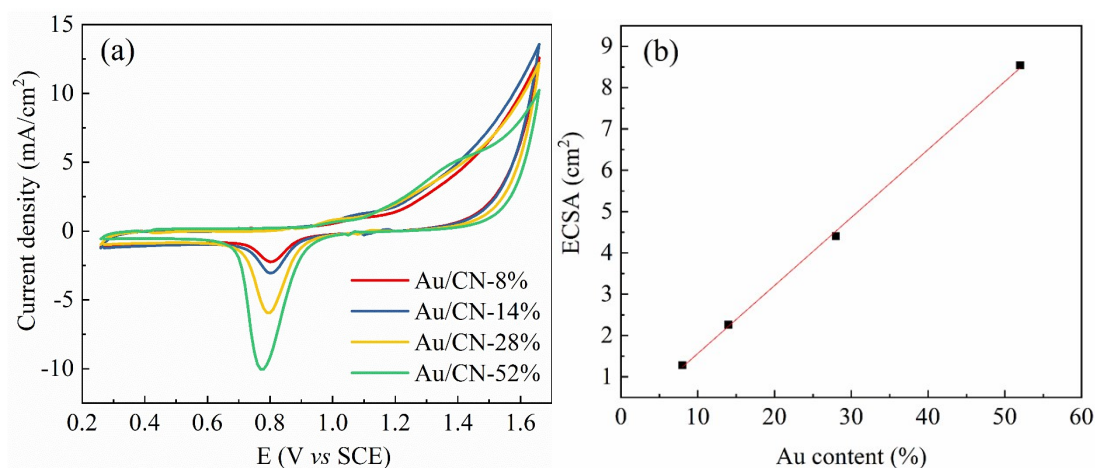


**Figure S6.** (a) CV curves of four Au catalysts in 0.1 M HClO<sub>4</sub> at the scan rate of 50 mV s<sup>-1</sup>; (b) ECSA differences plotted against gold content.

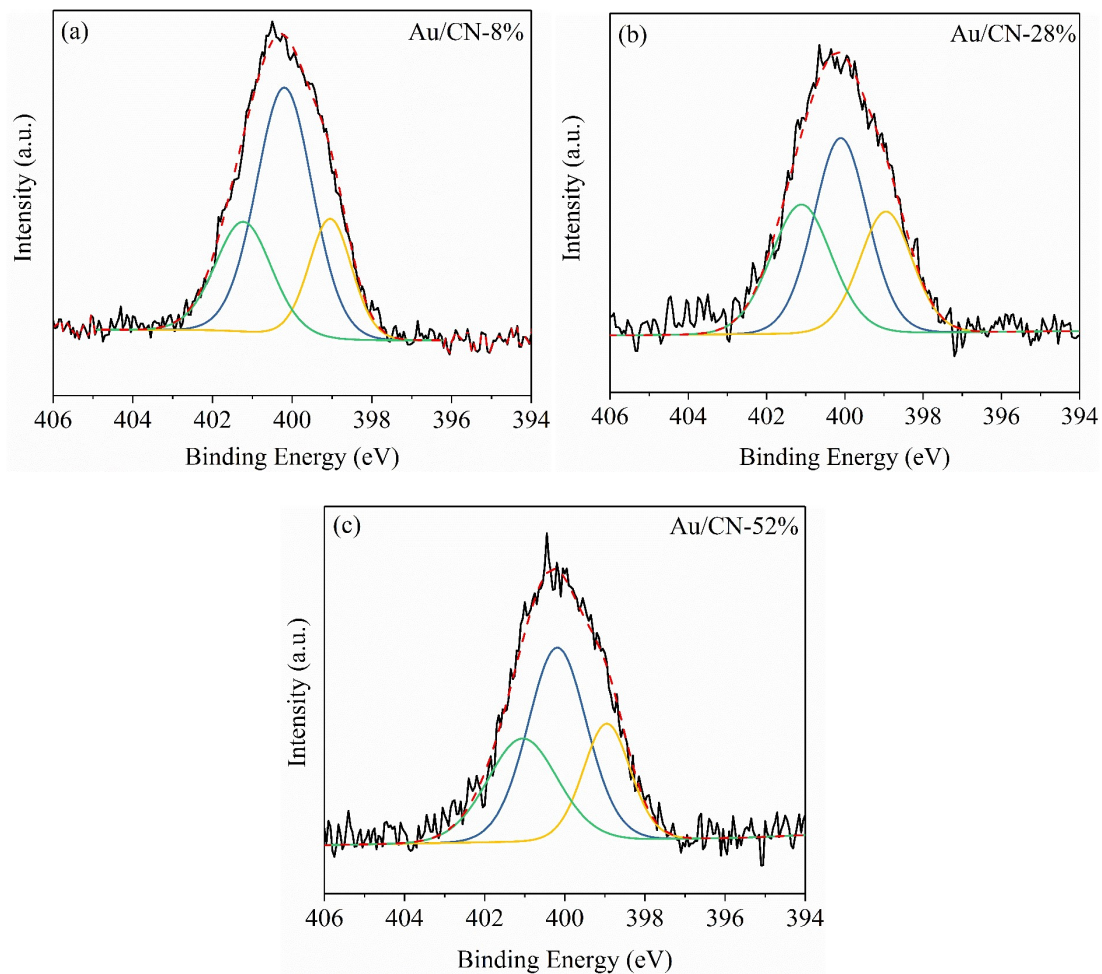


**Figure S7.** High-resolution N 1s spectra of three Au/CN catalysts.

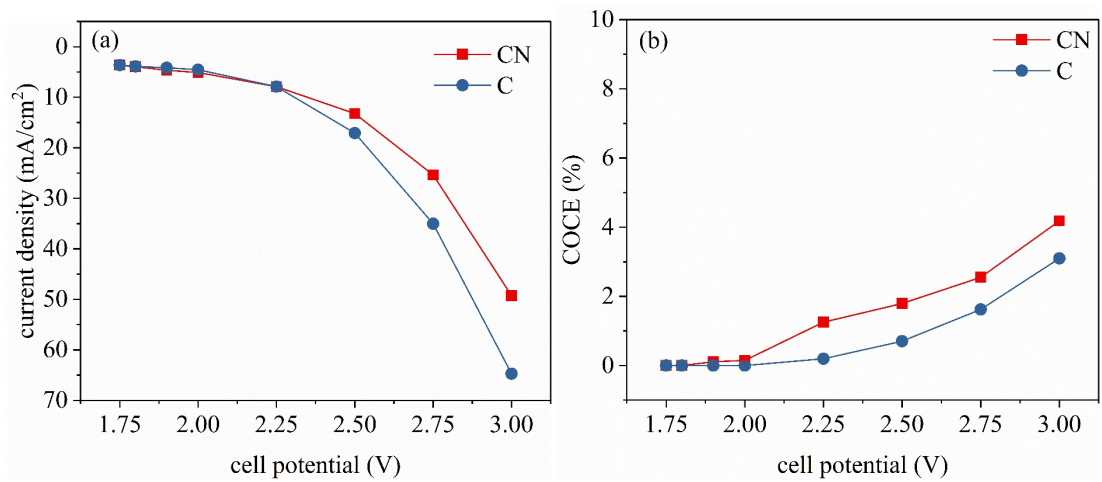


**Figure S8.** Cell performance of the C and CN was tested in the CO<sub>2</sub> electrolyzer. (a) average total current density and (b) current efficiency for CO production, as a function of the cell potential.



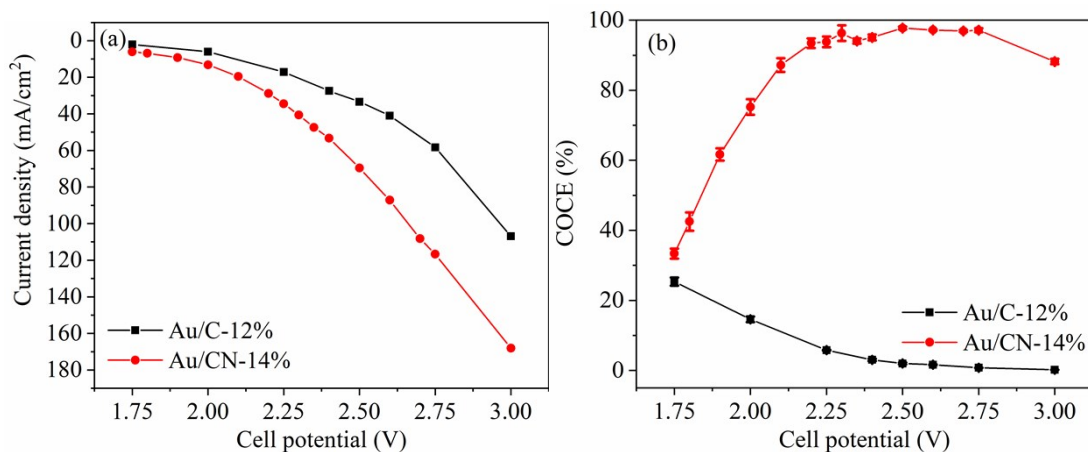


**Figure S9.** Cell performance of the Au/C-12% and Au/CN-14% tested in the CO<sub>2</sub> electrolyzer. (a) average total current density and (b) current efficiency for CO production, as a function of the cell potential.

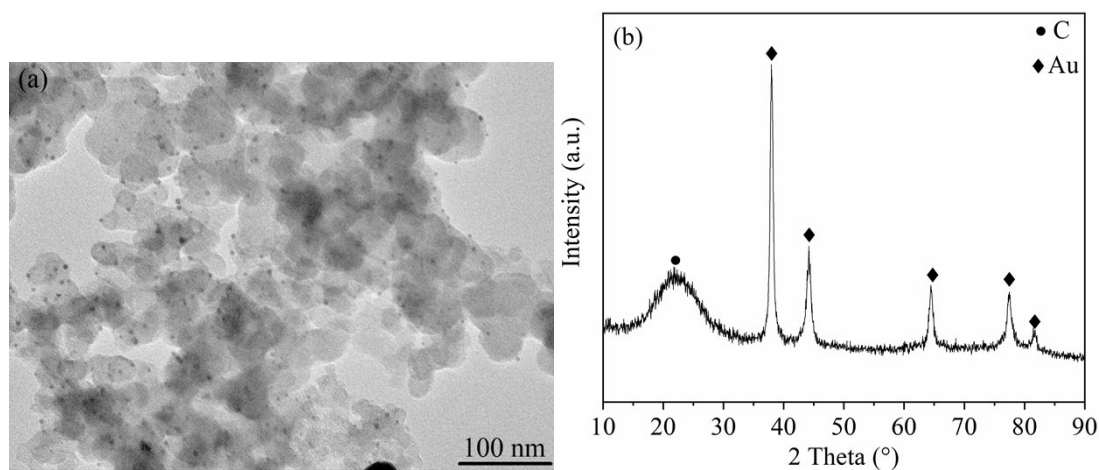


**Figure S10.** (a) TEM image and (b) XRD spectra of the Au/C-12% catalyst.

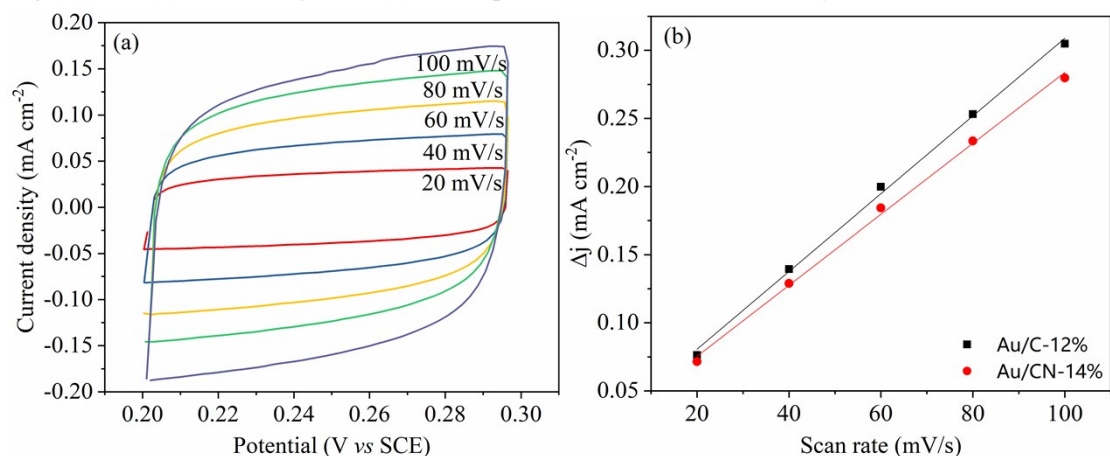


**Figure S11.** (a) CV curves of Au/C-12% catalyst measured at different scan rates in 0.1 M Na<sub>2</sub>SO<sub>4</sub> solution; (b) charging current differences plotted against scan rate.

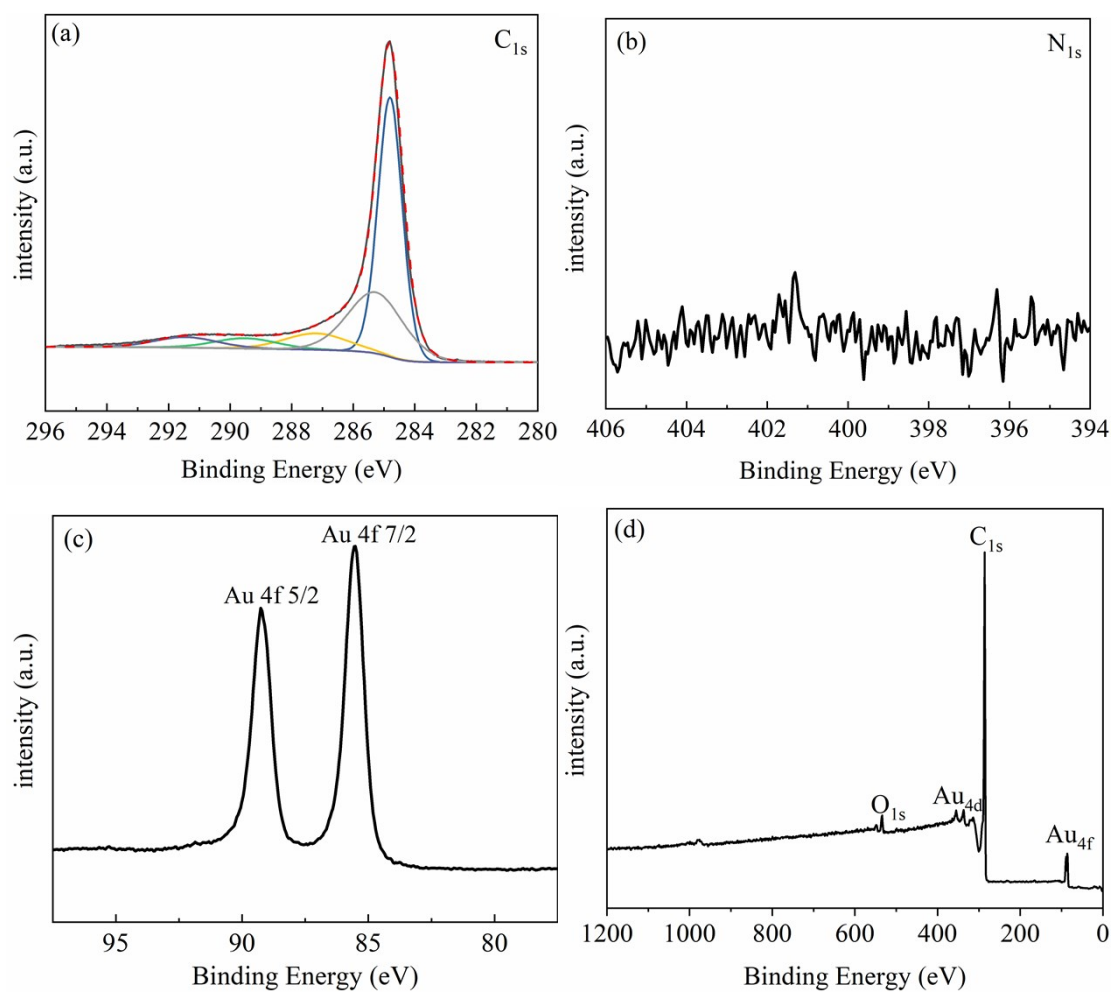


**Figure S12.** High-resolution C 1s (a), N 1s (b), Au 4f (c) spectra and XPS survey (d) of the Au/C-12%.

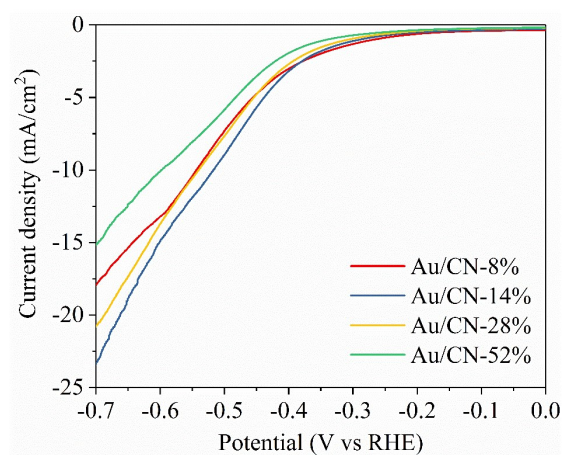


**Figure S13.** LSV curves at  $10 \text{ mV s}^{-1}$  in  $0.5 \text{ M KHCO}_3$  solution saturated with  $\text{CO}_2$  in H-cell.

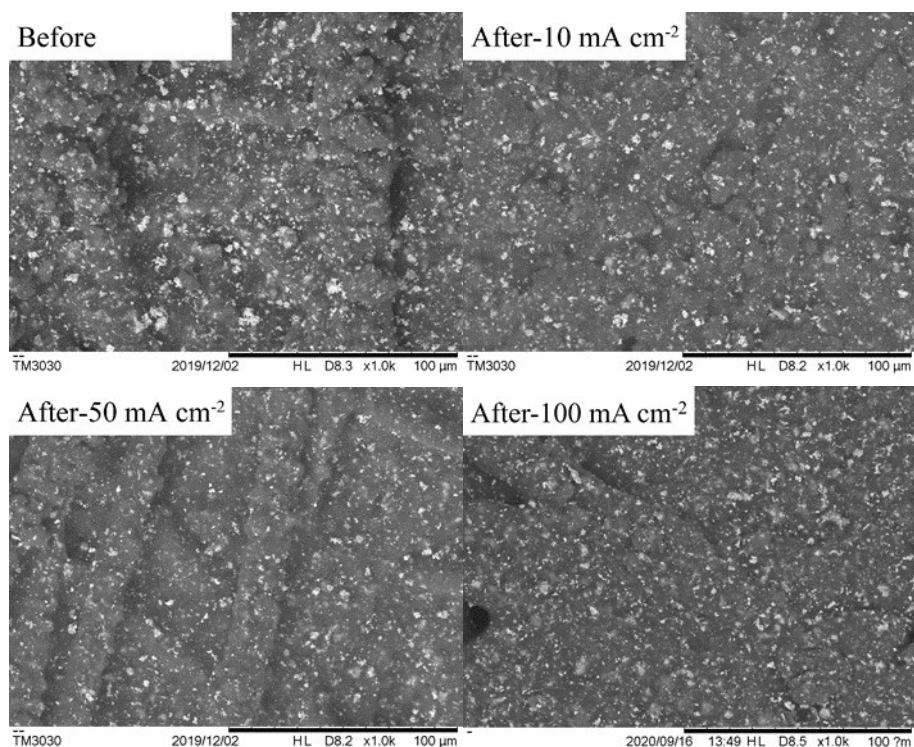


**Figure S14.** SEM image of the Au/CN-14% catalyst layer on cathode before and after stability tests at different current densities.

**Table S1.** XPS semi-quantitative analysis of the ratio of C and N in the four samples.

Sample	Composition (atomic %)	
	C <sub>1s</sub>	N <sub>1s</sub>
Au/ CN-8%	95.64	4.36
Au/ CN-14%	95.82	4.18
Au/ CN-28%	95.77	4.23
Au/ CN-52%	95.79	4.21

**Table S2.** Summary of reported CO<sub>2</sub> electrolyser's stability tests with gold catalyst.

Membrane	j <sub>CO</sub> (mA cm <sup>-2</sup> )	Potential (V)	COC E (%)	Temperatu re (°C)	Stability			Ref.	
					j <sub>total</sub> (mA/cm <sup>2</sup> )	COCE (%)	j <sub>CO</sub> (A /g <sub>Au</sub> )		Time (h)
AEM	~148	3.0	88	RT	50	>95	>339	130	This work
AEM	~425	3.0	>85	60	100	90-95	~230	100	1
None	~203	2.5	~65	RT	>111	>90	>556	8	2
None	~160	-1.78 V vs Ag/AgCl	>60	RT	~5	-	-	26*	3
CEM	~4	2.0	62	RT	~45	~70	~264	64*	4
CEM	~7	-0.7 V vs RHE	94	RT	~28	77	-	1	5

AEM, CEM, j<sub>total</sub> and RT represent respectively anion exchange membrane, cation exchange membrane, total current density and room temperature.

\* represents that the stability experiments were performed in half-cell.

1. Z. Yin, H. Peng, X. Wei, H. Zhou, J. Gong, M. Huai, L. Xiao, G. Wang, J. Lu and L. Zhuang, *Energy & Environmental Science*, 2019, **12**.
2. S. Verma, Y. Hamasaki, C. Kim, W. Huang, S. Lu, H.-R. M. Jhong, A. A. Gewirth, T. Fujigaya, N. Nakashima and P. J. A. Kenis, *Acs Energy Letters*, 2018, **3**, 193-198.
3. H.-R. M. Jhong, C. E. Tornow, C. Kim, S. Verma, J. L. Oberst, P. S. Anderson, A. A. Gewirth, T. Fujigaya, N. Nakashima and P. J. A. Kenis, *Chemphyschem*, 2017, **18**, 3274-3279.
4. Y.-H. Chung, M. G. Ha, L. Na, H.-Y. Park, H.-J. Kim, D. Henkensmeier, S. J. Yoo, J. Y. Kim, S. Y. Lee, S. W. Lee, H. S. Park, Y.-T. Kim and J. H. Jang, *Electroanalysis*, 2019, **31**, 1401-1408.
5. G. Park, S. Hong, M. Choi, S. Lee and J. Lee, *Catalysis Today*, 2019, **355**, 340-346.